Submitted to the International
Conference, Tbilisi USSR July 1976

FERMILAB-CONF-76-118-E

Measurement of the Pion Form Factor*

E. Dally, J. Hauptman, C. May, D. Stork
University of California at Los Angeles

J. Poirier, C. Rey, R. Wojslaw
University of Notre Dame

P. Shepard
University of Pittsburgh

A. Lennox, J. Tompkins, T. Toohig, A. Wehmann
Fermi National Accelerator Laboratory

I. Ioan, T. Nigmanov, E. Tsyganov, A. Vodopianov
Joint Institute for Nuclear Research, Dubna

ABSTRACT

A pion-electron elastic scattering experiment has been carried out at the Fermilab accelerator to measure the pion form factor. Negative pions in a 100 GeV/c beam were scattered from atomic electrons in a liquid hydrogen target. The trajectory of the incident pion and the scattering angles and momenta of both secondary particles were measured in a narrow angle magnetic spectrometer containing proportional chambers and magnetostrictive wire spark chambers. A sample of 10,000 elastic pion-electron events in the momentum transfer range $0.03 \leq q^2 \leq 0.07 (\mathrm{GeV/c})^2$ has been fit to a simple pole form factor. With a 2% uncertainty in the integrated cross section, we find a preliminary value for the pion radius of

$$\langle r^2 \rangle^{1/2} = 0.57 \pm .06 \text{ f.}$$

*Supported in part by U.S. Energy Research and Development Administration and the National Science Foundation

Measurement of the Pion Form Factor

The pion form factor has been measured in the momentum transfer range $0.03 \leq q^2 \leq 0.07 (\mathrm{GeV/c})^2$ by scattering pions from atomic electrons in a liquid hydrogen target. The pion form factor is defined to be the elastic scattering cross section divided by that predicted for a point pion. When it is expanded in powers of q^2, the mean-square radius of the pion electromagnetic charge distribution appears in the first coefficient:

$$\frac{d\sigma}{dq^2} = \left(\frac{d\sigma}{dq^2}\right)_{\substack{\text{POINT}\\ \text{PION}}} \left| F(q^2) \right|^2$$

$$= \frac{4\pi\alpha^2}{q^4}\left(1 - \frac{q^2}{q^2_{max}}\right)\left[1 - \frac{\langle r^2 \rangle}{6} q^2 + \ldots\right]^2$$

The experiment was performed in a 100 GeV/c negative pion beam incident on a 50 cm liquid hydrogen target at Fermilab. The maximum recoil electron energy is 84.0 GeV which corresponds to a maximum momentum transfer squared in the elastic reaction of $q^2 = 2\, m_e\, (E_e - m_e) = 0.086\ (\mathrm{GeV/c})^2$. These small momentum transfers give laboratory scattering angles which are typically a few milliradians within our acceptance. The experimental arrangement is shown in Figure 1. The trajectories of the incident pion and of the scattered pion and electron are measured with proportional wire chamber stations, each having four planes with 2 mm wire spacing staggered by 1 mm. The scattered particles are bent through two BM109 magnets with a total field integral of 70.35 Kg-m, and their trajectories beyond the magnets are measured by six magnetostrictive wire spark chambers.

Downstream of the spark chambers is a two particle trigger hodoscope. The geometric efficiency for triggering is nearly 100% for the q^2 range $0.03 \leq q^2 \leq 0.07 (\mathrm{GeV/c})^2$. An array of ten lead-glass shower counters 14 radiation lengths long served to reduce background triggers during the run and to aid in the subsequent indentification of elastic pion-electron events. Scattered muons were identified with a segmented steel filter.

An event trigger required conditions of two distinct types: the first was a beam monitor signal defining the incident pions. The beam logic was composed of information from scintillation counters and the proportional chambers upstream of the hydrogen target. A

portion of the beam logic required one and only one beam particle incident on the hydrogen target. This logic demanded a 1 microsecond spacing between usable particles; it vetoed beam counts with two particles in one r. f. bucket or with a particle in the following bucket. These requirements limited the amount of usable beam per machine pulse (typically, 300K particles through the spectrometer of which about 100K were usable for the experiment), but created a clean enviroment for spectrometer operation which removed serious ambiguities and inefficiencies from the trackfinding procedure.

The second trigger logic condition defined the pion-electron scatter: a two particle signature from the proportional chambers downstream of the target, a two particle signal from a scintillation counter array behind the spark chambers, and a Cerenkov pulse height consistent with that expected from the scattered electron. The trigger rate during data taking was about 1.4×10^{-4} per incident pion, and about 15 events were recorded during the 1 second machine spill.

The geometrical event reconstruction was done by finding tracks in the horizontal and vertical planes, and matching them in rotated chambers. The efficiency of pion-electron event finding has been tested both by monte carlo simulation of the experiment and by a second, independent program, and found to be 99.0±1.0% in this sample of data. A distribution of the reconstructed vertex position for elastic events is shown in Figure 2.

The pion-electron elastic scatters are separated from the large hadronic background by employing four constraints on energy-momentum conservation, and by requiring that the energy deposited in the lead-glass shower counters be consistent with the momentum measured in the spectrometer of the showering particle. Constrained chi-squared fits were performed on the spectrometer data for the pion-electron elastic reaction with an additional external bremsstrahlung photon assumed to be along the electron direction. The χ^2 distribution for this three-constraint reaction hypothesis on the present sample of data is shown in Figure 3; the tail on this distribution has contributions both from strong interaction background and from real pion-electron elastic scatters. A relatively large number of pion electron elastic events (about 3%) in this sample exceeds the statistical 1% confidence level (at χ^2=11.5 for three constraints), and these are accounted for by vertex associated radiative effects, pions which nuclear elastic

scatter in the target or the spectrometer matter, pions which decay inside the spectrometer, the non-gaussian distributions associated with plural scattering in thin absorbers, and systematics of the geometrical event reconstruction. The fitted bremsstrahlung spectrum is shown in Figure 4; the insert shows the spectrum near zero photon energy. The normalized and calibrated Cerenkov pulse height spectrum for kinematically identified elastic events is displayed in Figure 5.

The final separation of the elastic events from the background employs the geometry of event reconstruction in the target, the kinematic χ^2 from the constrained fit to elastic kinematics, a cut on the fitted bremsstrahlung energy at 4 GeV, and a minimum shower counter pulse height for electron identification. Specifically, we demand that the confidence level of the kinematic fit exceed the 10^{-6} level, that the shower counter pulse height exceed 50% of that expected for the electron, that the reconstructed vertex position be within 30 cm of the target ends, and that the kinematically fitted photon energy be between -2.0 and 4.0 GeV.

To obtain the form factor from the measured distribution in q^2 of elastic events, corrections for many physical and instrumental effects must be made. The principal corrections affecting the incident pion flux are pion attenuation in the target and spectrometer matter(2.87%), beam momentum cut from 96 to 102 GeV/c(3.02%), and muon contamination (0.40%). Principal corrections affecting the elastic sample of events are bremsstrahlung of the electrons(15% to 20%), pion attenuation (4.63%), and radiative corrections[1] (7.9% to 9.3%). The pion decay, muon-electron scattering, and strong interaction background corrections are less than 1%. Trackfinding efficiency was found to be 99%, and geometrical efficiency varied from 95.25% to 99.47%.

The corrected form factor is shown in Figure 6. At the present time a simple least squares fit which neglects error correlations has been carried out on this sample of data in order to provide a preliminary value for the pion radius. The fit is constrained in overall normalization to correspond to a 2 percent uncertainty in the absolute cross section. We find

$$\langle r_\pi^2 \rangle = 0.33 \pm 0.06 \text{ f}^2.$$

For comparison, vector dominance predicts 0.40 f^2, and the size of

the proton is 0.66 f^2. The first direct experimental determination[2] obtained 0.61±.15 f^2.

We express our appreciation to the staff of Fermilab for their assistance throughout this experiment. Dr. Charles Buchanan contributed to the preparation for the experiment, and Mr. Jonathan Kubic and Mr. Jim Volk were of great help. We are grateful for the support and encouragement of Dr. E. Goldwasser and Dr. A. Baldin.

References

(1) D. Yu. Bardin, G.V. Micelmacher, and N.M. Shumaiko, JINR E2-6235(1972)

(2) Adylov, et al., Physics Letters 51B,402(1974).

Figure Captions

Figure 1. The spectrometer layout in the M1 beam line in the Meson Lab. The beam line bends through 21 mrad with respect to the experiment center line.

Figure 2. The reconstructed vertex position in 10-cm bins of identified elastic scatters in the neighborhood of the 50-cm liquid hydrogen target. The ends of the vacuum region and the PWC stations 2 and 3 are visible.

Figure 3. The three-constraint chi-squared distribution for constrained chi-squared fits to the elastic reaction with an assumed bremsstrahlung photon along the electron direction.

Figure 4. The fitted bremsstrahlung spectrum for elastic events, with an insert showing this distribution near zero photon energy. The mean of this distribution is consistent with the known amount of matter which the scattered electron traverses.

Figure 5. The momentum normalized shower counter pulse height spectrum for elastic events.

Figure 6. The pion form factor.

B_0, B_1, B_2, A_H, A_5, SeSp — Scintillation Counters
All PWC Stations = 2X planes, 2Y planes
(R) = Rotated chamber(s)
(Transverse Dimensions are not to scale)

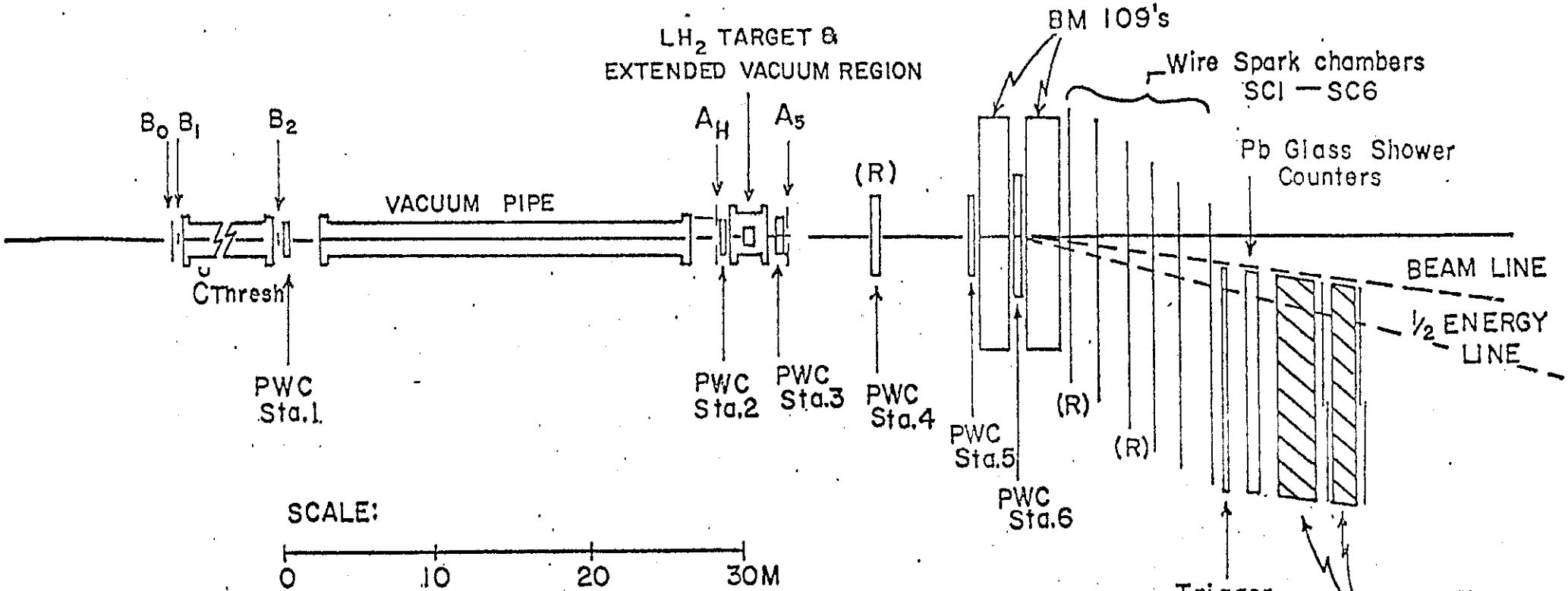

SPECTROMETER LAYOUT

Figure 1.

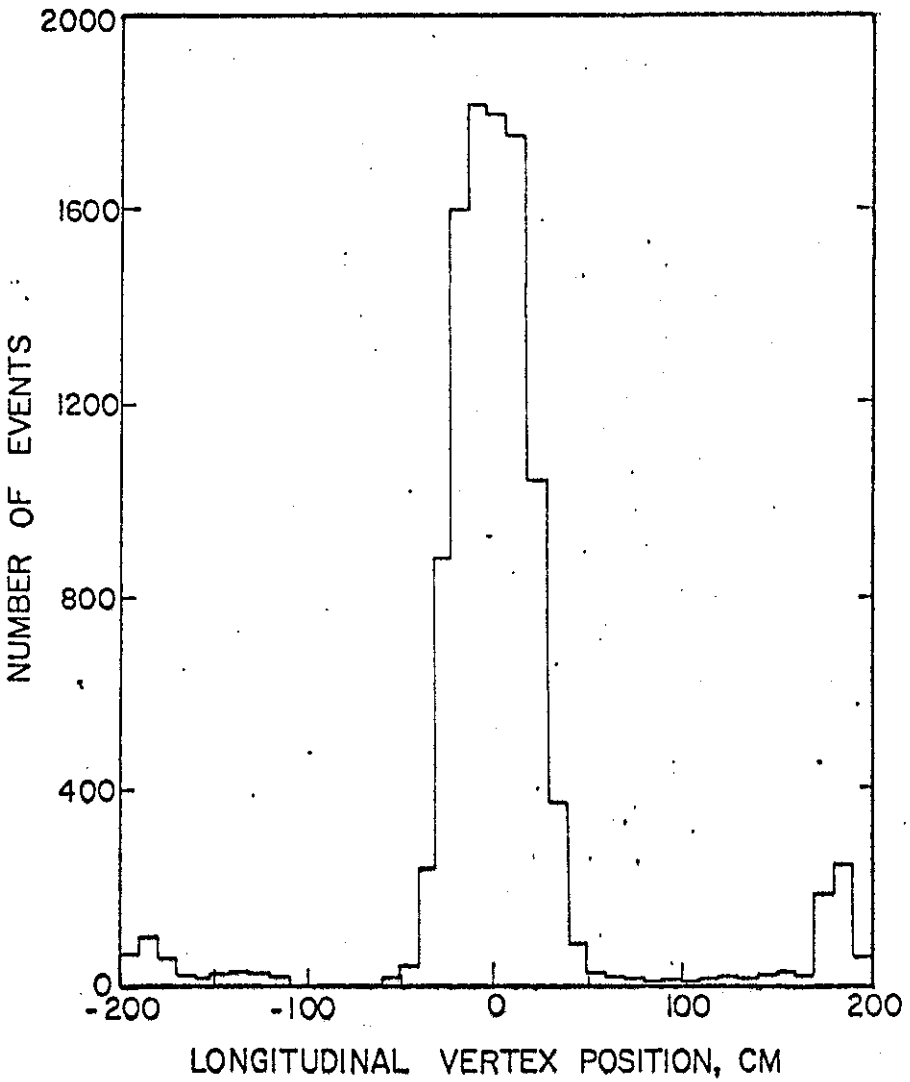

Figure 2.

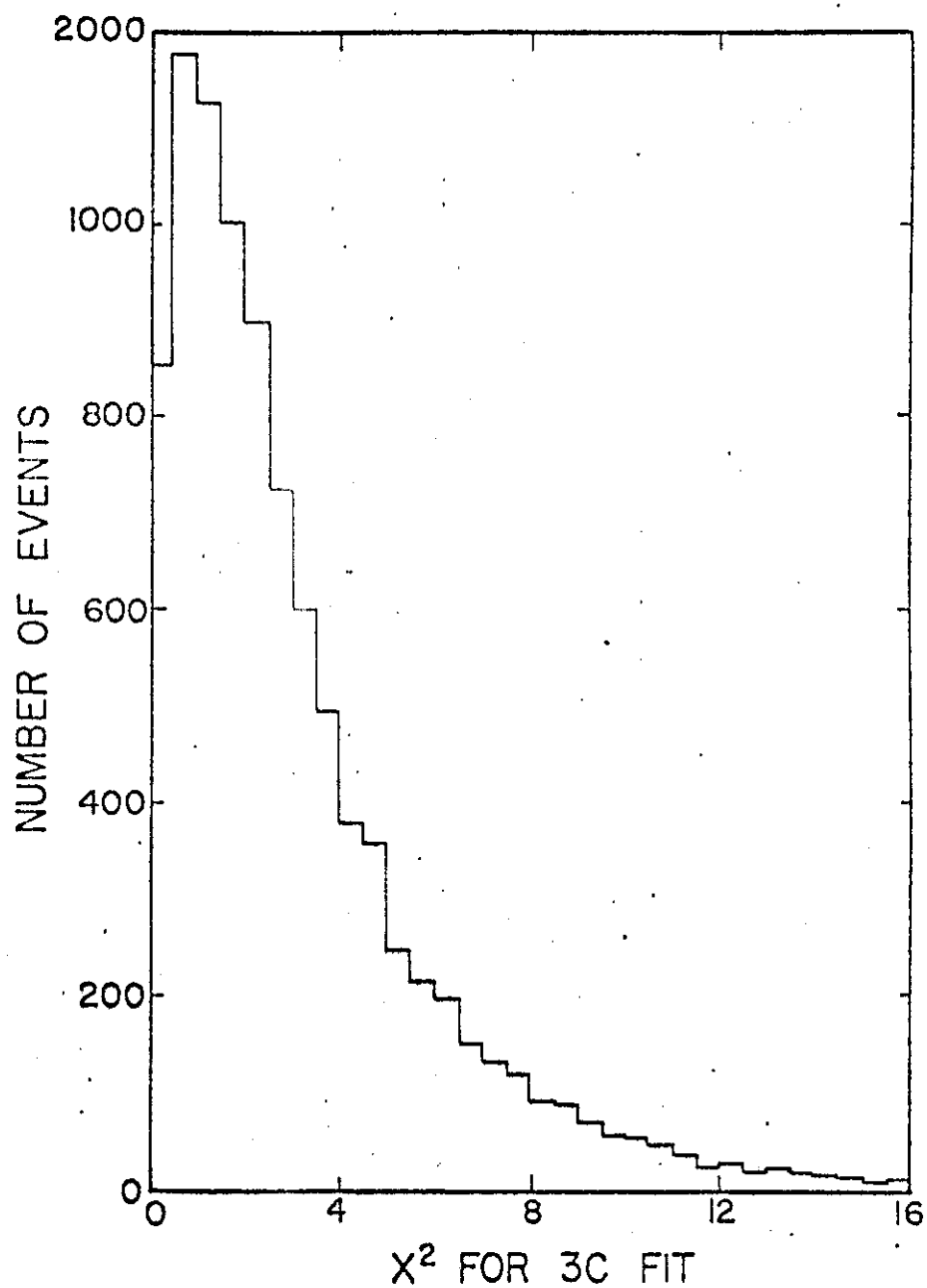

Figure 3.

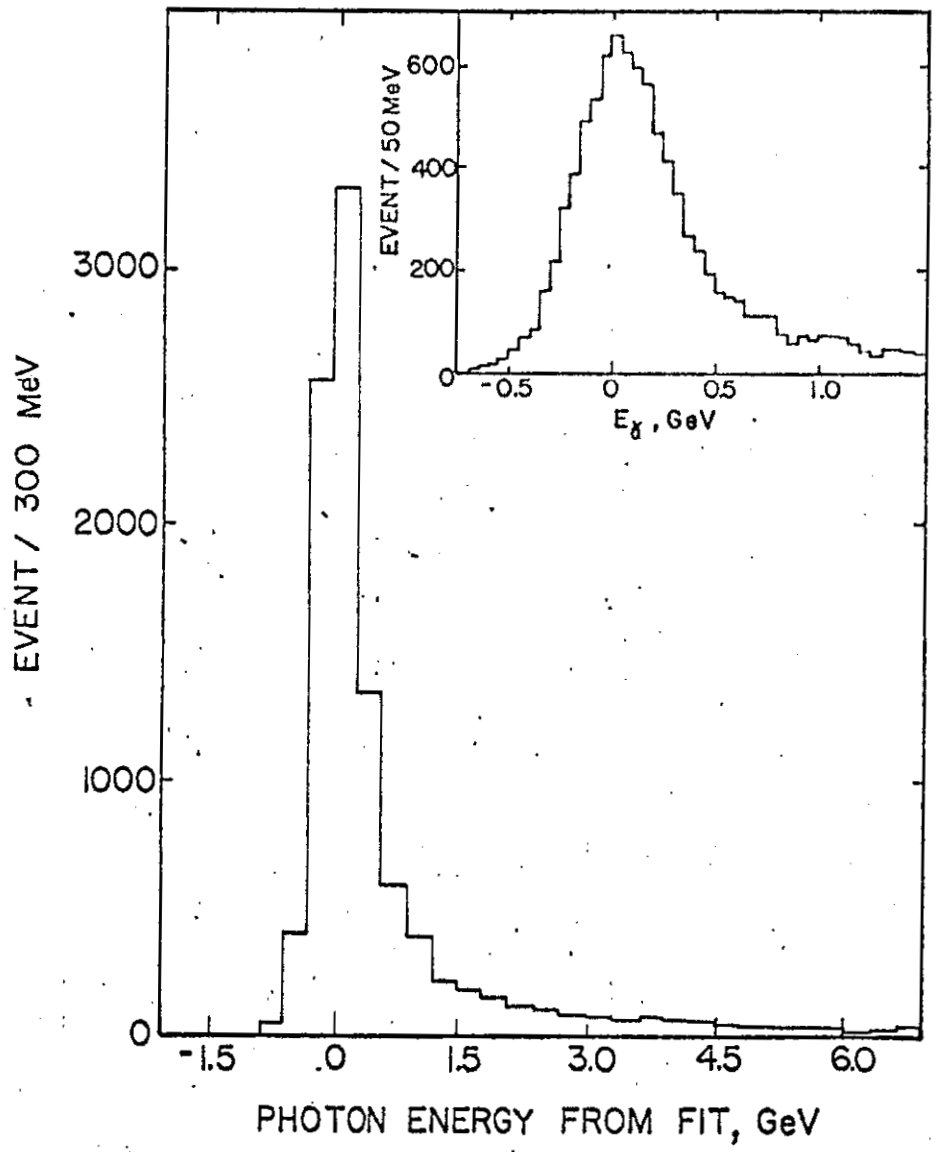

Figure 4.

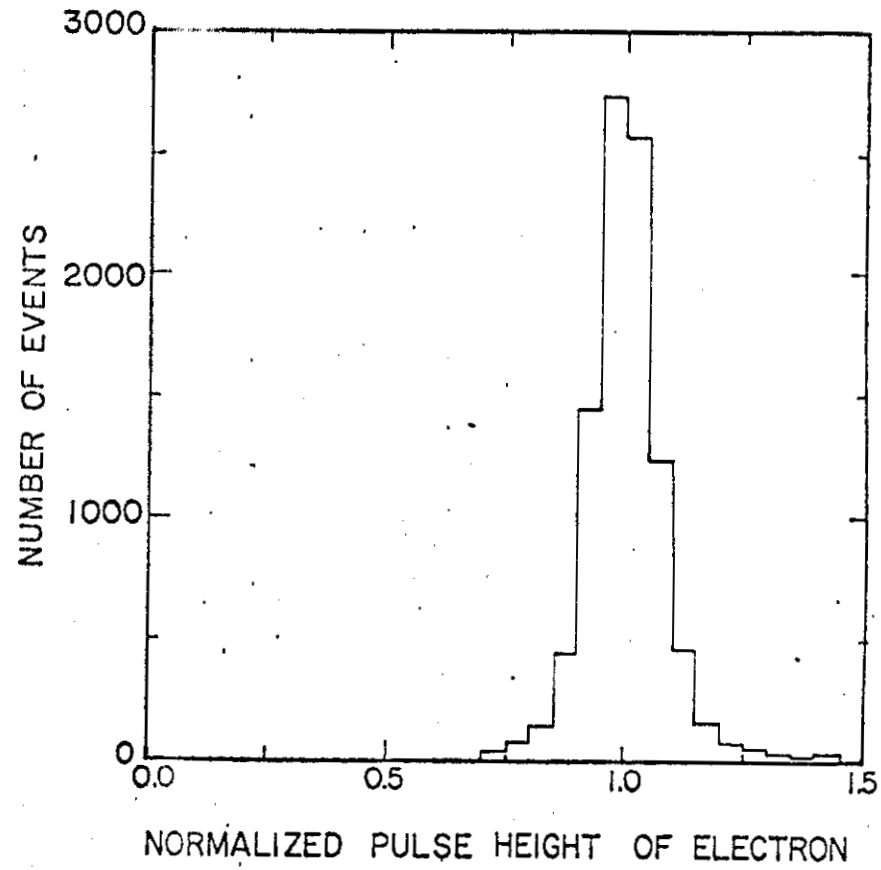

Figure 5.

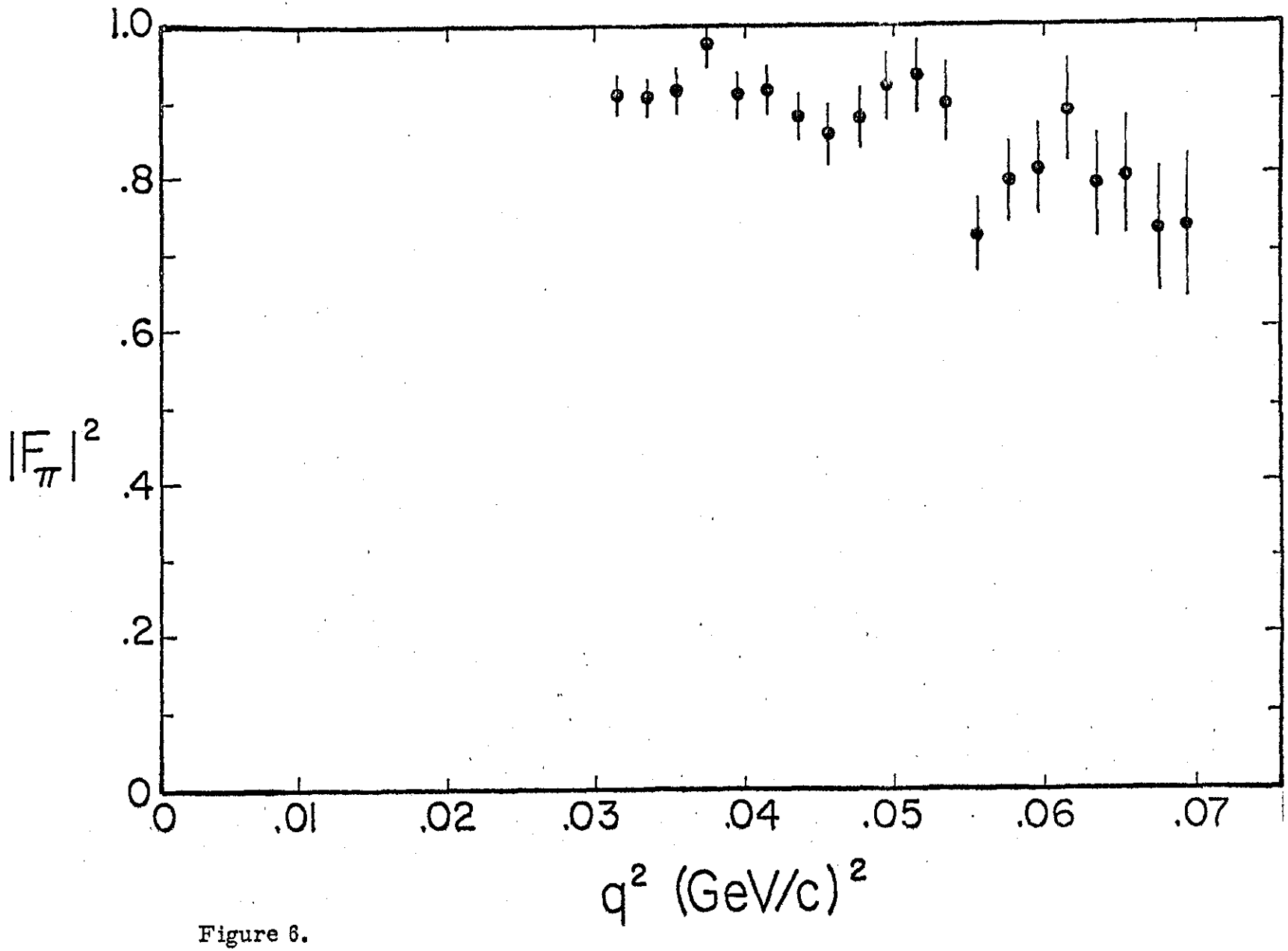

Figure 6.